

CHAPTER VI

OBSERVATION RESULTS AND CONCLUSION

This radio telescope system is constructed, but the thesis cannot be considered to be complete without the observation. At first, the observation site and the treatment is described. Since the data is saved in binary file, the preliminary survey of the effective noise is displayed graphically. The last and summit of the thesis is the result of the observation.

Observation Site and Treatment

The observation is taken in the rural area of Muak Lek district, Saraburi Province. The geographic position of the site is Long. $101^{\circ}12'13.33''$ E and Lat. $14^{\circ}39'38.57''$ N. Since the site is considerably free from the uncontrollable tremendous man-made noise of the big city and have the sufficient stable electrical power, it is our choice.

The operated frequency of the system is 110 MHz. Since the bandwidth of the system is 183 kHz and the receivable FM radio broadcasting station at the site is about 90 MHz, it can be considered that there is no effects from the FM broadcasting signal. However, there may be some problems from the amateur radio communication which is a station in that area. The problem is not important since the station is long distance

(about 1 km) and the main beam of the antenna is oriented far from that station. Moreover the operation is not full time and avoidable.

The antenna mounting is the equatorial type and fixed to the meridian. The polarization is arranged to be vertical. Since the position of the main beam is fixed, the position of the source at the transit time can be calculated by the expressions in chapter II. The equatorial coordinate of the source at the transit time is provided in the day of observation from the program EZCosmos. The main beam deviation is compensated.

The selected sampling rate is 128 SPS which the recorded data for 1 sector of the hard disk correspond to the integer value of second. The sampling rate is suitable for the size of storage media to hold the data of the rate 900 KB/hr.

The recorded data is converted back to the power by the measured parameters from the last chapter. The brightness temperature of the system can be found by the expressions from chapter II and the assumptions that the temperature distribution is constant over the source and independent of frequency in the predetection bandwidth. By the receiver calibration, The brightness temperature of source is the different between the antenna temperature and the receiver temperature.

The source of interest is the Sun. However the useful survey of the local noise is valuable. The next section is dedicated to it.

Local Noise Survey Results

the first observable noise is from the system arrangement itself. From the experiment, if the computer is placed near the antenna, the tremendous induced noise

is occurred only when someone is moving near the field since the high sensitivity of the system. This problem can be eliminated by the separation of the antenna and another apparatus. However, there are some noise from hard disk which can be observed from the recorded data but disappear when monitor directly. The noise from hard disk observed in 4 second is displayed in the Fig 6.1. The effect of the digital low-pass filter of $N = 64$ with the different cut-off frequency F_c can be seen also in the same figure. This occurrence of this noise is about 4 times per sec and can be eliminate effectively by the digital low-pass filter at cut-off frequency the 3 Hz.

The dominated man-made noise which is detectable is from the vehicle. Although the site is far from the road, the vehicle of the local resident have some effect, especially in the morning when the most people go to work. However, the effect for a vehicle is occurred in small fraction of time (less than 1 minute) and vanish after it pass. The Fig. 6.2 show the equivalent temperature when the motorcycle riding pass the antenna. The three pattern are produced in 1 minute and filtered for elimination the noise from hard disk. It is clearly that the patterns are similar but the width of the pattern since the difference of passing speed.

There are another man-made noise which is not dominate and can be avoidable such as the switching of the electrical component in vicinity. For the natural interference, the interference from thunderstorms is also detected as shown in Fig 6.3. It can be seen the transient noise when there are thunderbolt.

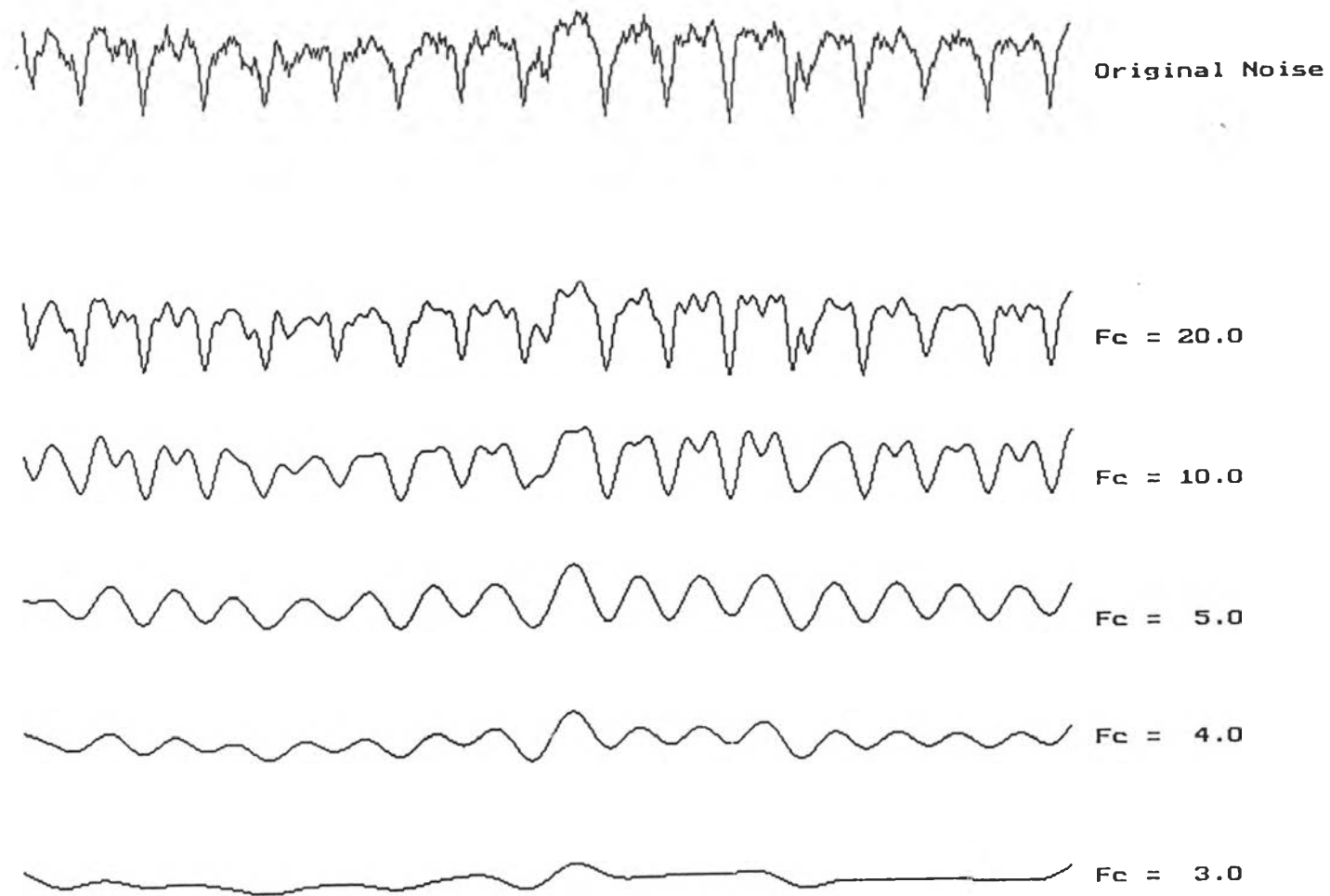


Fig 6.1 Noise from operation of the hard disk and effects of the filter with difference cut-off frequency in Hz

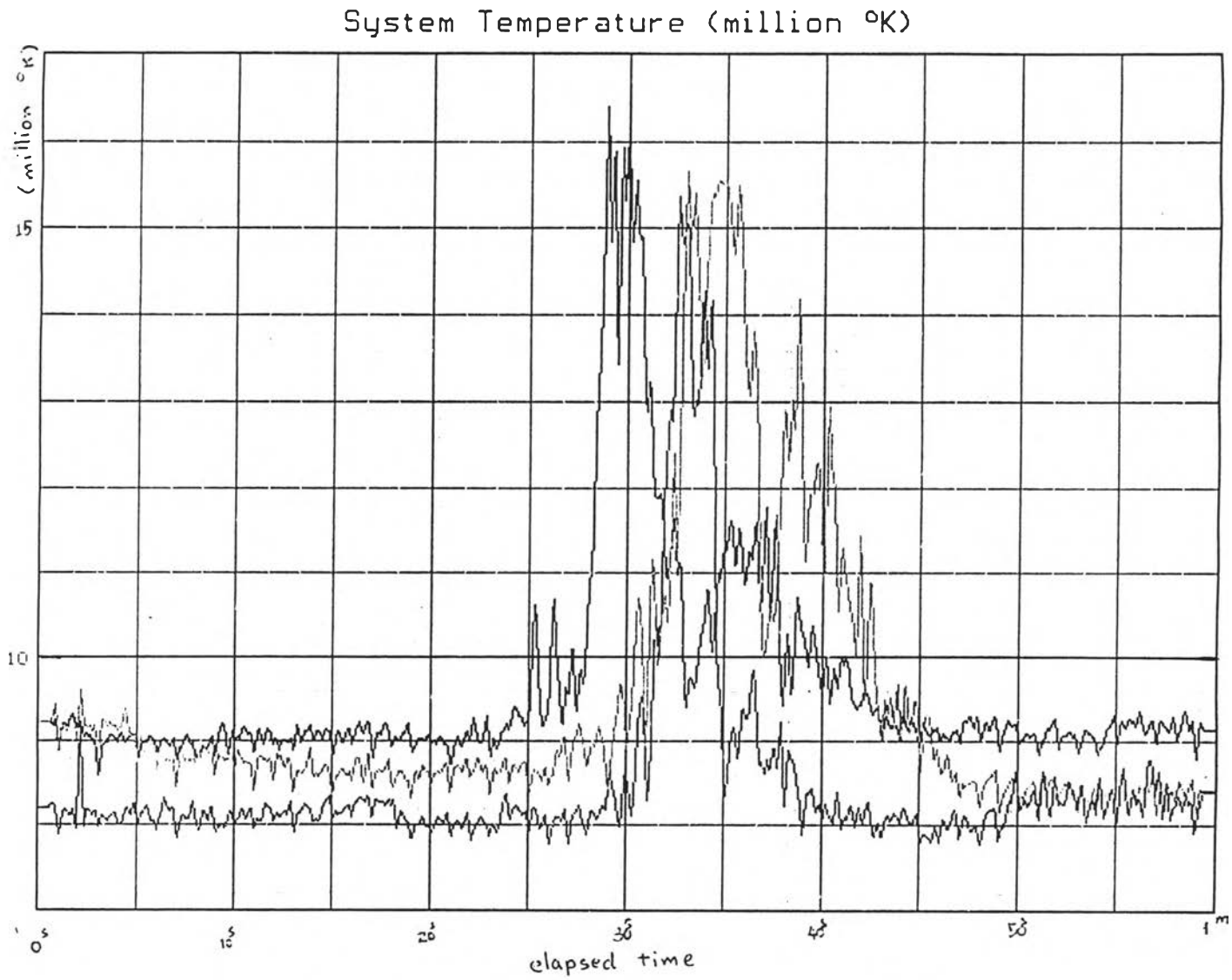


Fig 6.2 System temperature from the passing motorcycle.

System Temperature (million °K)

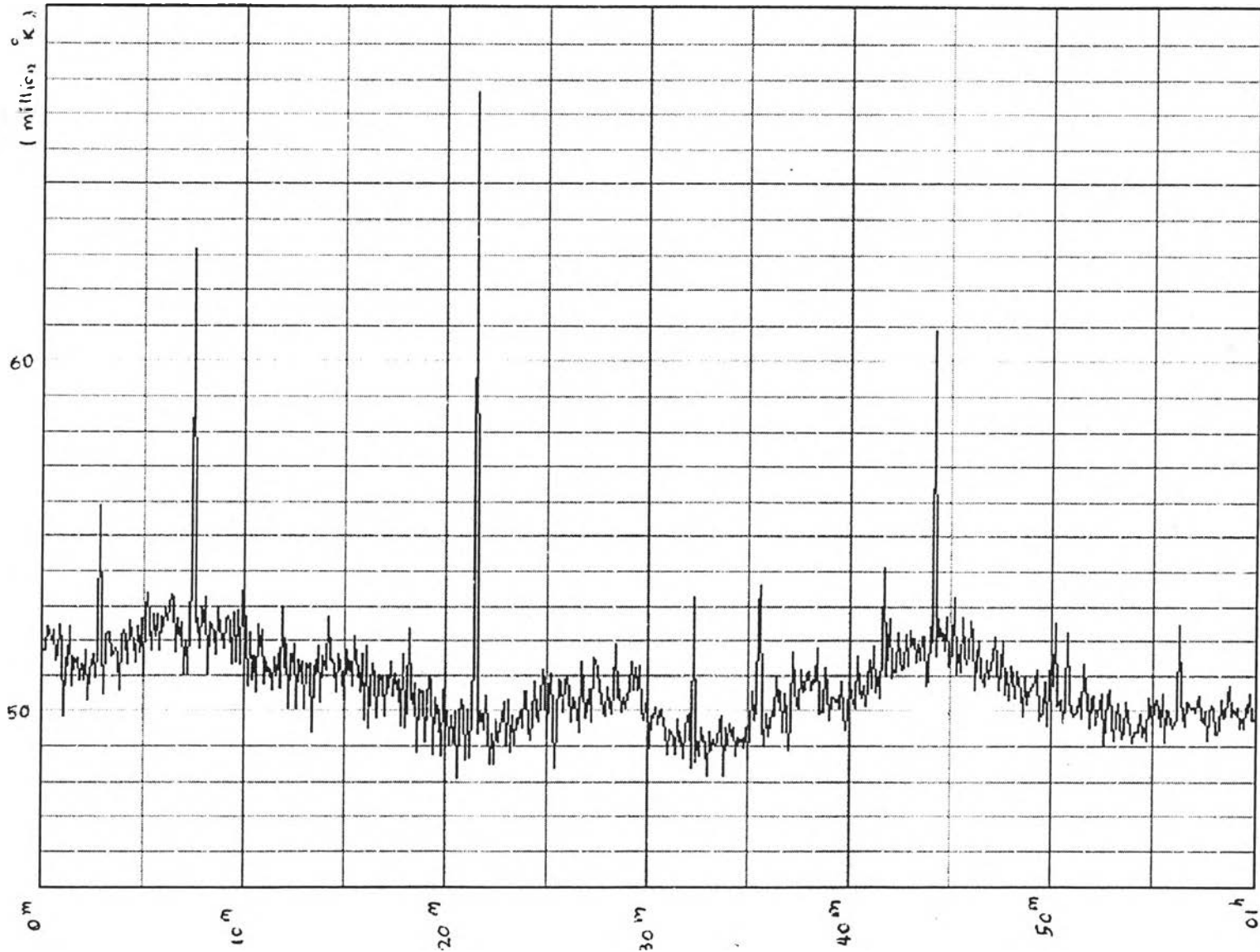


Fig 6.3 System temperature detected in thunderstorms.

System Temperature (million °K)

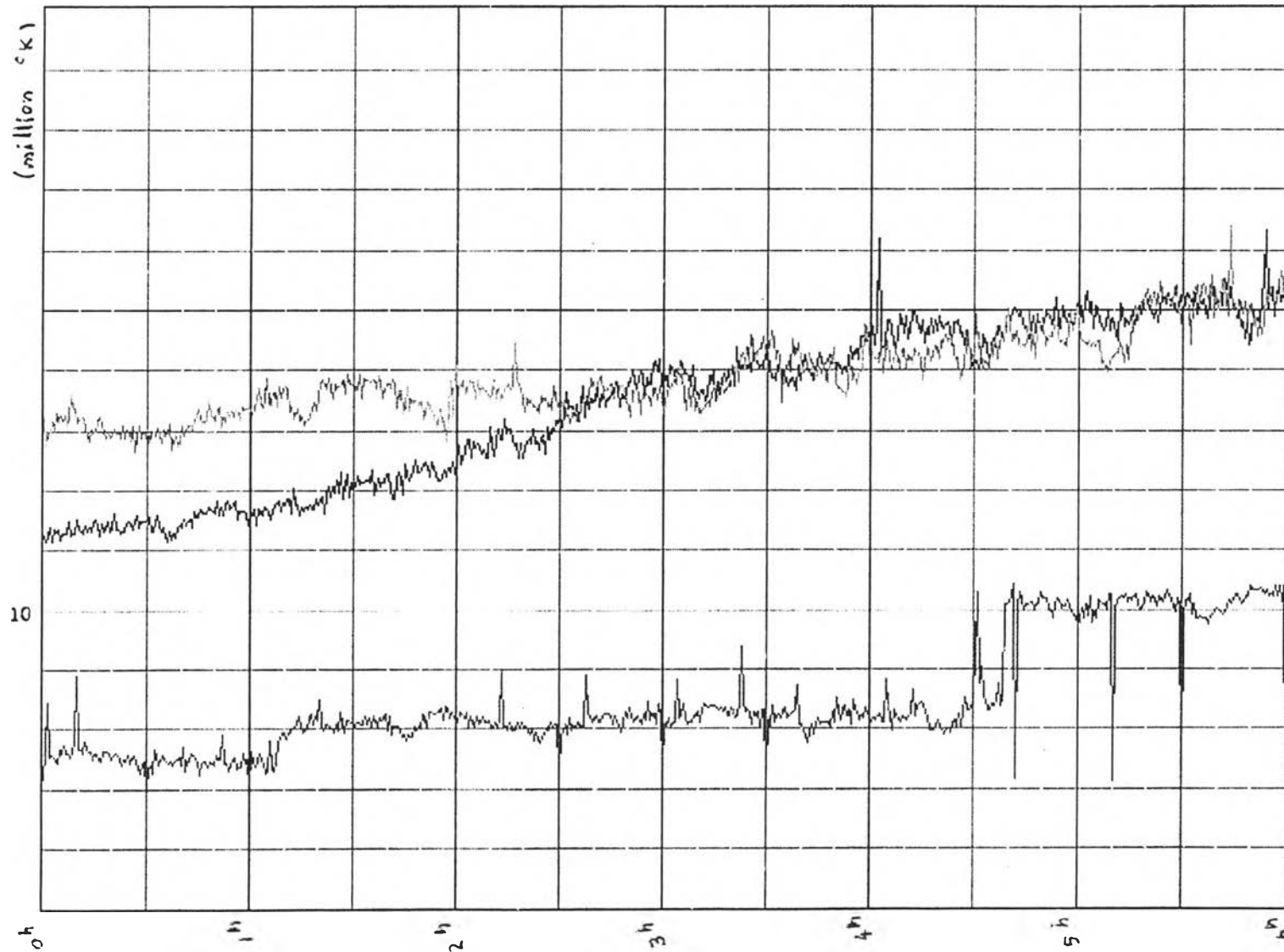


Fig 6.4 Drift pattern of the receiver temperature.

The most problem of the observation is come from the drift of system. The drift is occur in both gain and offset. Although the drift of the offset can be recover by the calibration process but the drift of gain in the measured equipment cannot be corrected. The Fig 6.4 show the receiver temperature at difference condition in 6 hr MST. The most drifting rate is measured in the daytime and the second is the same but cool down by electric fan throughout the observation time. The lowest signal and also lowest drift is measured in the night without cooling. Note that the increasing at the last of this record is come from man-made in the morning and can be neglected. It can be referred that the cause of the long-term drift is temperature. The other measured data which gathered in the night with the electric fan may confirm this phenomena. The drifting rate have not significant different to the data measured without the electric fan which is according to the fact that the temperature in the night is not significant difference whether the fan is used or not.

Observational Result

Now we have the sufficient information for observation the celestial objects by our radio telescope. The celestial object which is test the performance of our system is the Sun. The reason behind the selection is that the sun is the visible object which is one of the most brightest object in radio frequency.

The sample of the system temperature in difference day is shown in Fig 6.5 to Fig 6.7. The record time is the Thai standard time and total observation time is 6h--MST which center is corresponding to the transit time. Hence the BWFN of the antenna is about 20 degree, the time of the Sun passing the main beam is about 1^h 20^m

MST. Since the signal from the source situated at the main beam have varies slowly, the sampling rate (128 SPS) cannot degrade the information of the measurement data. The measured data is filtered by the parameters $N = 64$ and $F_c = 3$. It mean that the integration time is 1 second. The digital code is converted to the temperature scale. The calibrations for receiver temperature can be seen in each graph. From (2.17), the antenna temperature is the subtraction of the system temperature and the receiver temperature.

Conclusion and Discussion

We were constructed a radio telescope system which is controlled by a personal computer. The advantage of the system are the automatic acquisition and accurate signal processing. The physical quantities can be estimated easily and precisely comparing to another read-out devices. By aid of appropriate digital filter, the signal to noise ratio is tremendously improved as seen in Fig.6.1 .

However, it can be seen that the result is not according to the expectation that the signal should be appear as the pattern of the antenna with peak at the center of the graph. It is clearly seen the effect of the drift in the record. The result cannot be interpreted as the signal from the Sun. However, The noise survey confirm the fact that the system can be used to measure the small signal from many source, but the long-term recording suffers from the thermal drift. However the result should be compared with the other observation. The blackbody temperature of the sun at difference frequency is shown in Fig. 6.8 .

System Temperature (million °K)

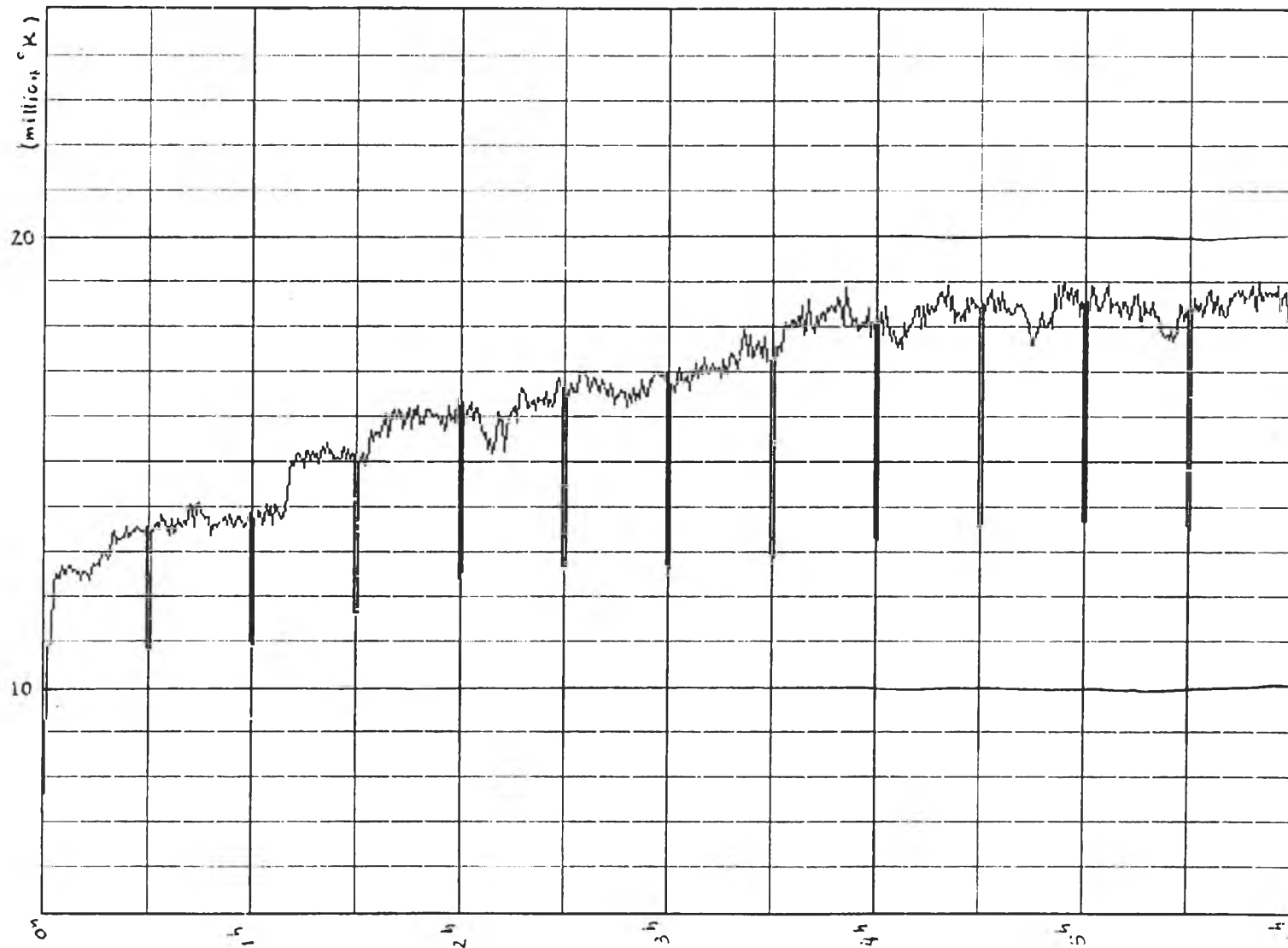


Fig 6.5 System temperature observed in 22-Mar-1997 between $10^{\text{h}}02^{\text{m}}2.39^{\text{s}}$ - $16^{\text{h}}02^{\text{m}}2.39^{\text{s}}$

System Temperature (million °K)

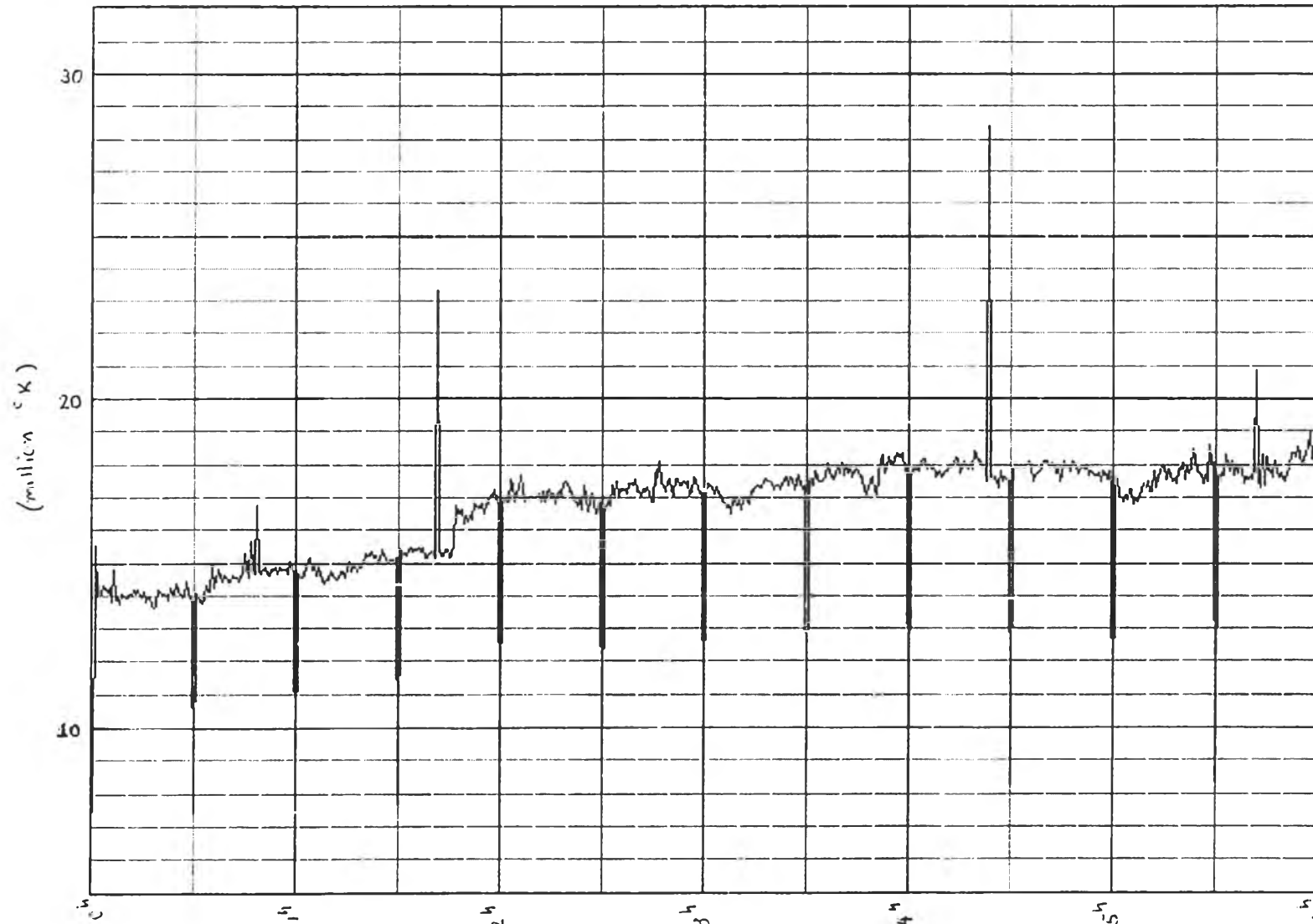


Fig 6.6 System temperature observed in 23-Mar-1997 between 10^h01^m43.89^s - 16^h01^m43.89^s

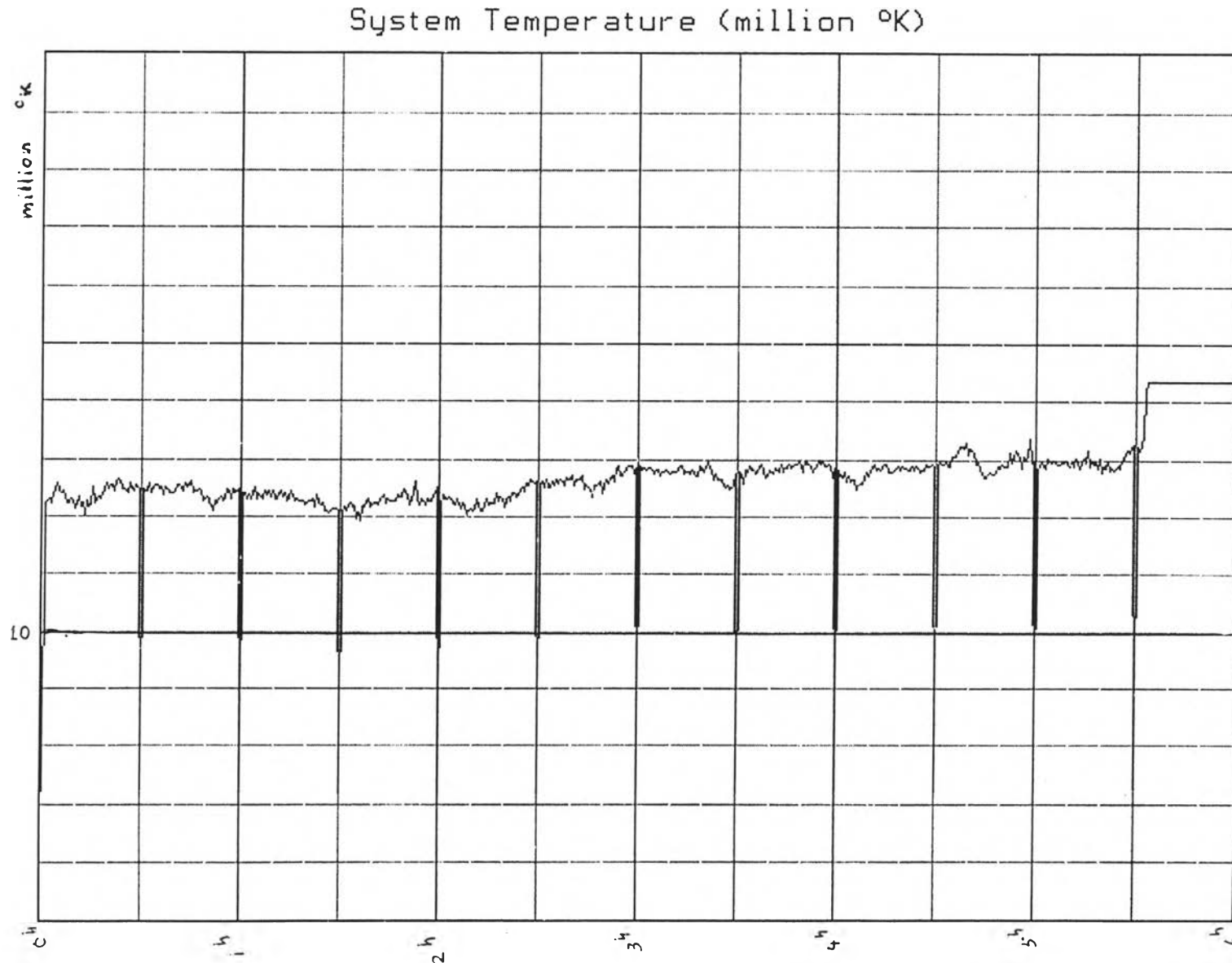


Fig 6.7 System temperature observed in 24-Mar-1997 between $10^{\text{h}}01^{\text{m}}25.38^{\text{s}}$ - $16^{\text{h}}01^{\text{m}}25.38^{\text{s}}$. The last of signal have the problem from power line.

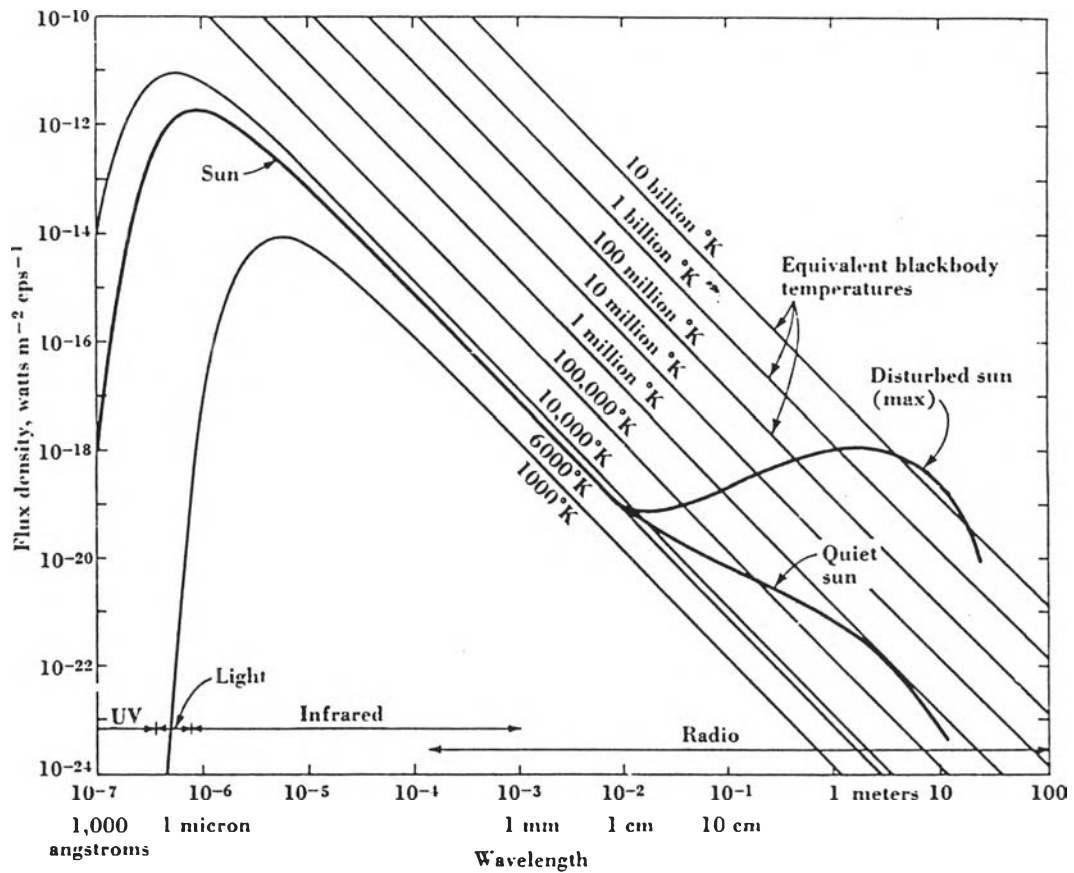


Fig 6.8 Temperature of the sun at difference wavelength (Kraus,1986).

The observation were made in the time of the quiet Sun and the operating frequency is 110 MHz (wavelength is about 2.73 m). According to Fig 6.8, the Sun have the equivalent temperature about 1 million Kelvin of blackbody. Compare to the antenna temperature from the previous results are vary in order of 1-10 million Kelvin and can be varied in order of 0.01 to 10 since the uncertainty of the RF gain as discussed in the chapter V and the linear relation of the power and temperature as derive in the chapter II. Hence, the measured value can be considered to be the same order of the previous observation.